Eur. Phys. J B **18**, 257–261 (2000)

THE EUROPEAN PHYSICAL JOURNAL B

EDP Sciences

Asymmetric local displacements in the $Bi_2Sr_2CaCu_2O_{8+\delta}$ superconductor

N.L. Saini[1], A. Lanzara[1], A. Bianconi[1,a], and H. Oyanagi[2]

[1] Unita' INFM and Dipartimento di Fisica, Università di Roma "La Sapienza", P.A. Moro 2, 00185 Roma, Italy
[2] Electrotechnical Laboratory, Umezono, Tsukuba, Ibaraki 305 Tsukuba, Japan

Received 5 June 2000

Abstract. Instantaneous in-plane Cu–O bond distribution in the $Bi_2Sr_2CaCu_2O_{8+\delta}$ (Bi2212) superconductor has been investigated by high k-resolution Cu K-edge extended X-ray absorption fine structure (EXAFS) measured with polarized vector parallel to the two orthogonal Cu–O–Cu bonds of the CuO_2 square plane. The results show an anisotropic Cu–O distribution in the two directions and provide further information on the local atomic displacements in the lattice-charge stripes.

PACS. 74.72.Hs Bi-based cuprates – 61.10.Ht X-ray absorption spectroscopy: EXAFS, NEXAFS, XANES, etc. – 74.80.-g Spatially inhomogeneous structures

1 Introduction

Recent advances in experimental techniques and materials synthesis have given a new direction towards a same platform to understand the physics of doped perovskites. In fact superconductivity in cuprates and colossal magnetoresistance (CMR) in manganites appear in a novel inhomogenous phase of condensed matter with the interplaying lattice, charge and spin degrees of freedom [1,2]. There have been a number of experimental and theoretical reports on coexisting two component [3–8], where one of them is made of charges associated with local atomic displacements: polarons and/or charge density waves [9–16]. The segregation of the two component at mesoscopic scale gives a complex phase with charge carriers ordered in striped domains [17–20].

While it has been easier to solve the local atomic displacements in doped manganites being larger, results on doped cuprates, with smaller disorder, have shown ambiguity on the magnitude of the atomic displacements depending on the time scale of the experimental techniques used. However, clear evidences of electronic and lattice instabilities in these materials are beyond discussion and it is now getting recognized that the lattice excitations indeed play important role in the physics of high T_c superconductors. Recent experiments on the isotope effect [21–23] have further demanded the need to include the electron lattice interaction as one of the parameters to describe the complex metallic phase of the cuprate superconductors.

The contribution of X-ray absorption spectroscopy (XAS) has been vital due to availability of high brilliance and polarized X-ray synchrotron radiation sources allowing to get directional information around a selective site. Recently the polarized Cu K-edge XAS has been successfully exploited to obtain local and instantaneous displacements around the Cu site in high T_c cuprates, as the CuO_2 plane is an important ingredient to drive electronic properties of these materials [24–28]. Using in-plane and out-of-plane polarized EXAFS, providing Cu–O pair radial distribution functions, in combination with the diffraction measurements, giving the superlattice wavevector, we have found that there are Jahn-Teller distorted Cu sites (Q_2-mode) which get ordered in stripes and coexist with undistorted sites [29–33].

$Bi_2Sr_2CaCu_2O_{8+\delta}$ (Bi2212) has been one of the suitable systems to observe the lattice-charge stripes and to investigate their implication to the electronic structure [34]. In fact the Fermi surface of this system shows broken segments at the M points due to asymmetrically suppressed spectral weight because of lattice-charge stripes [34]. In addition, the Fermi surface obtained by angle resolved photoemission spectroscopy (ARPES) shows large anisotropy in the two orthogonal M points, (*i.e.*, two orthogonal Cu–O–Cu bond directions) with appearance of an additional spectral weight only along one direction with small $k_F = 0.2 \pm 0.03\pi$ and energy dispersion $\Delta E \sim 80$ meV [35].

It is worth recalling that the structure of Bi2212 has orthorhombic symmetry where the perovskite axis is along the Cu–O–Cu bonds (usually called tetragonal axis) and the diagonal axis (45° from the perovskite axis) is along the Cu–Cu direction (also called orthorhombic axis). Recently we have shown that the lattice distortions in the stripes are quite complex and anisotropic [36] showing different Cu–O pair distribution along the diagonal axis and in the perovskite axis. Furthermore, we have shown quadrupole contribution of $1s \rightarrow 3d$ ($\Delta l = 2$) transition in the Cu K-edge XANES of the Bi2212, having

[a] e-mail: antonio.bianconi@romal.infn.it

maximum intensity when polarization vector of the synchrotron light is parallel to the diagonal axis and minimum intensity when polarization is along the perovskite axis (*i.e.*, Cu–O–Cu bond direction). The present work is motivated by the observed anisotropy of the Fermi surface in the two orthogonal M point directions [34,35] and the anisotropic local lattice displacements in the diagonal and perovskite axes. We have further exploited the capabilities of polarization dependence of the Cu K-edge EXAFS, providing directional pair distribution function (PDF), in combination to the angular dependence of the quadrupole transitions, allowing to identify the Cu–O–Cu directions. This approach is applied jointly with high k-resolution EXAFS spectra obtained with a high signal to noise ratio to investigate the directional PDF of the CuO_2 plane in the Bi2212 system. The results clearly show a strong anisotropy of the Cu–O bond distribution in the two orthogonal Cu–O–Cu bonds directions and provide a direct evidence for preferential tilting of the CuO_2 plane in the diagonal lattice-charge stripes. The results are consistent with the ARPES data showing asymmetric spectral weight distribution at Fermi surface in the M directions [34,35].

2 Experimental

A well characterised monocrystal of $Bi_2Sr_2CaCu_2O_{8+\delta}$ (Bi2212), grown by the traveling solvent floating zone (TFSZ) method was used for the measurements. The polarized Cu K-edge absorption measurements at room temperature were performed on the beamline BL13B of Photon Factory at High Energy Accelerator Research Organization in Tsukuba [37]. The synchrotron radiation emitted by a 27-pole wiggler source (maximum field B_0 of 1.5 T) inserted in the 2.5 GeV storage ring with a maximum stored current of 360–250 mA was monochromatized by a newly installed variable exit beam height double crystal Si(111) monochromator and sagittally focused on the sample. Improved lattice of the storage ring and better monochromator cooling system allowed to have very stable beam on the samples. The spectra were recorded by detecting the fluorescence yield (FY) using a 19-element Ge X-ray detector array. In addition, the large number of detectors have allowed us to cover a large solid angle of the X-ray fluorescence emission. The emphasis was given to measure the spectra with a high signal to noise ratio and up to a high momentum transfer ($Q = 2k = 38$ Å^{-1}), and for the purpose we have measured several scans, with each scan averaged over 19 channels. The well oriented crystal was mounted on a Huber 420 goniometer with colinearity of the sample normal and the azimuthal rotation axis within $\pm 0.5°$, established by laser alignment prior to the measurements and further controlled by the laser and telescope mounted on the goniometer. The grazing incidence geometry was used for the measurements by keeping the electric vector of the synchrotron light parallel to two orthogonal Cu–O–Cu bond directions selected by pre-edge peak intensity representing $1s \rightarrow 3d$ quadrupole transition having minima when the polarization is falling flat on the Cu–O bond (*i.e.*, $3d_{x^2-y^2}$ lobes).

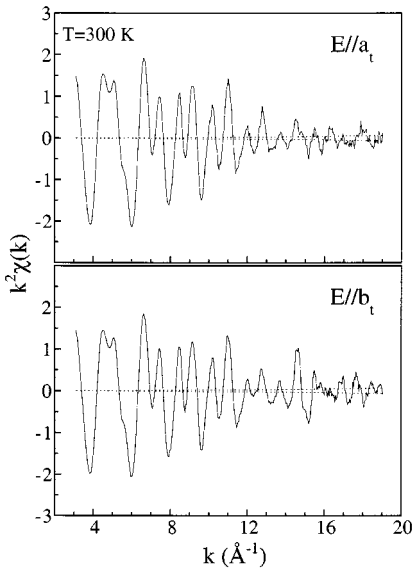

Fig. 1. Polarized Cu K-edge EXAFS extracted from the absorption spectra measured on an optimally doped $Bi_2Sr_2CaCu_2O_8$ single crystal at 300 K with polarization vector of the synchrotron light parallel to the two orthogonal Cu–O–Cu directions ($E \parallel \mathbf{a}_t$ and $E \parallel \mathbf{b}_t$). The noise level is shown as dotted lines. The EXAFS spectra are shown multiplied by k^2.

One of the common problems with EXAFS measurements on single crystals is Bragg glitches due to sample diffraction peaks. Generally these Bragg peaks are easier to remove by taking away the affected channels of the multielement detector. However, in the present case, since the sample alignment is well known and the experimental set-up allows different geometrical freedom (the incidence angle, the detection angle and distance) the geometry has been selected in such a way that any Bragg peak due to diffraction are out of the detector window, within the scan energy range. The incidence angle of $\sim 2°$ with respect to the surface was found to be suitable, keeping the centre of the detector window siting orthogonal to the beam direction, at around 30 cm away from the sample, with an angle of about 20° from surface of the sample. This common geometry was used for recording all the absorption spectra. A standard procedure [38] was used to extract the EXAFS signal from the absorption spectrum. The EXAFS spectra have been corrected for the X-ray fluorescence self-absorption [39].

3 Result and discussion

Figure 1 shows EXAFS signals extracted from Cu K-edge absorption spectra of Bi2212 crystal measured at room temperature (300 K) with E vector of the plane polarized X-rays falling parallel to the two orthogonal Cu–O–Cu bond directions of the CuO_2 square plane, *i.e.*, two perovskite axes of the crystallographic unit cell (hereafter called $E \parallel \mathbf{a}_t$ and $E \parallel \mathbf{b}_t$ spectra). The signals are multiplied by k^2 to emphasize the higher k-region. Inspite of damping of the EXAFS signal due to Debye-Waller

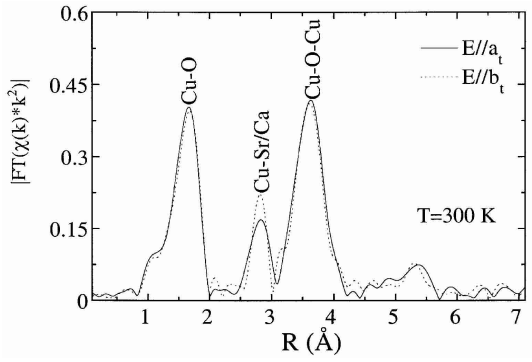

Fig. 2. Magnitude of the Fourier transform $|\mathrm{FT}(k^2\chi)|$ of the EXAFS spectra measured in the $\mathbf{E} \parallel \mathbf{a}_t$ (solid line) and $\mathbf{E} \parallel \mathbf{b}_t$ (dotted line) geometries. The FT are performed between $k_{\min} = 3$ Å^{-1} to $k_{\max} = 19$ Å^{-1} using a Gaussian window and not corrected for the phase shifts due to photoelectron backscattering.

factors at 300 K the EXAFS oscillations are visible upto $k = 19$ Å^{-1} out of the experimental noise level (the dotted lines). This suggests that EXAFS with a high k-resolution could be well exploited to study complex systems even at higher temperatures if measurements are made with a high signal to noise ratio, reducing both random error and a systematic noise. The difference in the EXAFS oscillations could be clearly seen in the figure. It should be mentioned that the two spectra were recorded in a sequence and therefore with similar experimental conditions and a similar treatment was given to extract the EXAFS signals suggesting that the differences are intrinsic to the sample.

The differences in the R-space could be seen in the Fourier transform (FT) of the two EXAFS signals (Fig. 2). Peaks in the FT appears due to backscattering of the emitted photoelectrons from neighbouring atoms and hence the FT provides global atomic distribution around the absorbing site (around Cu in the present case). The peaks in the FT do not represent the real atomic distances and the position should be corrected for the photoelectron backscattering phase shifts to find the quantitative value to the atomic positions with respect to the Cu atom. There are evident differences in the FT of the EXAFS spectra measured along the two polarizations with major differences around the Cu-Sr/Ca peak. The Cu–O peak in the $E \parallel b_t$ appears to be shifted towards higher R while the Cu–O–Cu peak shows a shift towards lower R-value. On the other hand, the Cu-Sr/Ca peak shows a large increase and gets sharpen in the $E \parallel b_t$ geometry. The anisotropy in the distribution of Sr/Ca atoms suggests a large redistribution of Cu-Sr/Ca bonds and complex distortions of the lattice. Although absolute differeneces may be difficult to extract due to complex interference effects of different backscatterings of the photoelectrons, the evident differences are large enough to state that the PDF is anisotropic with respect to the two Cu–O–Cu directions. In fact the FT of the EXAFS signals in the two directions have demonstrated clearly the anisotropy of the Cu–O bonds along the two orthogonal directions.

Anisotropy along the two orthogonal Cu–O bond directions was quantified by modelling the EXAFS spectra. For this purpose, we have used similar approach as discussed in our earlier papers on high T_c superconductors and related perovskites [29,40,41]. Let us recall that there are several factors which should be taken into account to obtain precise information on the atomic displacements in the CuO_2 lattice by analysing the Cu–O EXAFS signal. The main problem comes from drastic damping of the Cu–O backscattering at the high k-values. The problem is further enhanced at room temperature because of damping due to bigger Debye-Waller factors and the small Cu–O signal could be easily masked by the experimental noise. Nevertheless, the solution of the lattice displacements is limited by the k-resolution and there could be further damping of signal because of distribution of distances *i.e.* $\Delta R_{\min} = \pi/2k_{\max}$. The problem is more complicated when the EXAFS is measured on a powder sample due to reduction of the effective coordination number and spatial averaging, however, this could be taken care by measuring single crystal samples with well defined directions selected by the polarization of the synchrotron light (as the present case). Considering the limitations we have measured the EXAFS spectra with a high k-resolution and with a high signal to noise ratio by accumulating a large number of scans limiting to the noise level to the order of 10^{-4} (Fig. 1). Therefore improved experimental conditions could allow to extract the Cu–O EXAFS oscillations with high k-resolution and to study precise local lattice displacements in the CuO_2 plane.

The in-plane Cu–O PDF was obtained by the analysis of the EXAFS signal due to the Cu–O backscatterings. Figure 3 shows the PDF of CuO_2 plane along the two orthogonal Cu–O bond directions. Since EXAFS measures correlated distribution in a locally ordered structure, we have used correlated distance broadening of the Cu–O bonds to determine the PDF [40]. The resulting distribution lies in the range of 1.8–2.05 Å independent of the polarization direction. The PDF obtained in the $\mathbf{a}_t$ direction at 300 K is compared (middle panel) with the PDF obtained by analysis of the EXAFS spectra measured in the same direction at low temperature (30 K). The bond distribution well reproduces our earlier results at low temperature [36], however, due to larger distance broadening at higher temperature the PDF at 300 K show an asymmetric distribution of Cu–O bonds instead of clear two peak function at 30 K. The large distribution of the Cu–O distances along the two orthogonal directions within the CuO_2 plane evidently shows distorted nature of the square plane.

We have also shown the distribution of Cu–O bonds measured by anomalous diffraction in the Bi2212 system (lower panel) [29]. The overall bond distribution lies in the range of 1.8–2.05, consistent with the EXAFS measurements. However, the diffraction distribution is averaged over all the sites while the EXAFS distribution represent directional distribution.

The PDF along the two Cu–O–Cu bond directions are different. While the Cu–O distribution along the $E \parallel \mathbf{b}_t$ is a single (however broad) peak function centered around the average bond length (~ 1.9 Å), the distribution along

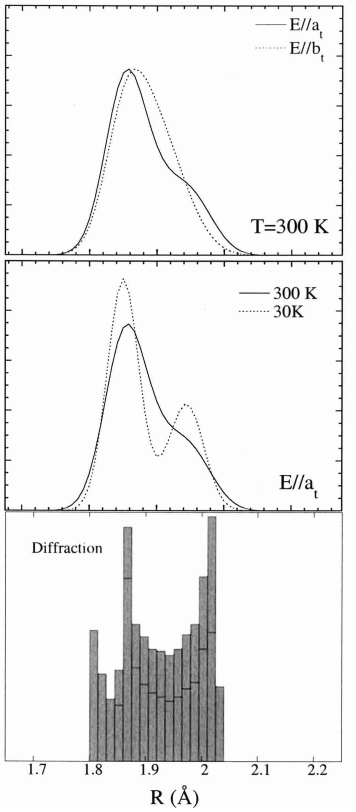

Fig. 3. Pair distribution functions (PDF) of the CuO_2 plane in the two orthogonal direction of the Cu–O–Cu bonds (upper). The PDF are determined from the EXAFS spectra due to Cu–O pairs while the E vector of the polarized light is $\mathbf{E} \parallel \mathbf{a}_t$ (solid line) and $\mathbf{E} \parallel \mathbf{b}_t$ (dotted line). The PDF in the $\mathbf{E} \parallel \mathbf{a}_t$ (solid line) direction at 300 K is compared with that of at 30 K in the same direction (middle). The distribution of Cu–O bonds measured by Cu K-edge anomalous diffraction [29] in the Bi2212 system is also shown for comparison (lower).

the $E \parallel \mathbf{a}_t$ appears with more like a double peak function appearing respectively at $\sim$ 1.88 Å and $\sim$ 1.98 Å. The PDF evolves in a clear two peak function at low temperature as shown in the midde panel of Figure 3 comparing the PDF along $\mathbf{a}_t$ direction at 30 K and 300 K. The outcome of the present experiment, shown as PDF at 300 K, not only indicates anisotropy of the Cu–O distribution in the CuO_2 square plane but also provides an evidence for preferential tilting of the CuO_2 plane giving higher probability of longer and shorter bonds arranged in one of the Cu–O–Cu directions. This observation is consistent with the electronic anisotropy of the $\Gamma-M$ and $\Gamma-M_1$ directions at the Fermi surface of the Bi2212 system [35] and further supports the important role of local lattice in electronic excitation spectrum of the complex systems such as high T_c superconductors.

A large number of experiments have shown that highly distorted CuO_2 square planes coexist with the undistorted ones and get ordered in lattice-charge stripes along the diagonal direction (Cu–Cu direction, *i.e.*, 45° from the Cu–O–Cu bond direction) with segregation of itinerant and relatively localized charges [29–33]. A cartoon picture of the stripes is shown in Figure 4 where the circles represent CuO_2 sites. The circles with arrows are highly distorted CuO_2 sites while empty circles are undistorted CuO_2 sites (or Cu sites with small distortions). The lattice-charge stripes have a periodicity of about 9 Cu-sites along the diagonal direction as shown by several diffraction experiments on the same system. The present experiment adds further information and suggests preferential tilting of the CuO_2 planes, indicated by arrows pointing towards tilt direction, with higher probability of shorter and longer Cu–O bonds in the $\mathbf{a}_t$ direction. In addition, the preferential tilt gives reduced periodicity by a factor of two due to instantaneous lattice fluctuations. Recently anomalous phonon dispersion has been interpreted as dynamic unit cell doubling in the CuO_2 plane along the direction of Cu–O–Cu bonds giving a short range charge ordering [42]. The present experiment can account the dynamic unit cell doubling in the CuO_2 plane along the direction of the Cu–O–Cu bonds as argued on the basis of the anomalous phonon dispersion. Therefore, the dynamic unit cell doubling of the CuO_2 plane or "half breezing mode" appears to be due to intra-lattice-charge stripe fluctuations in the wide stripes [29–33].

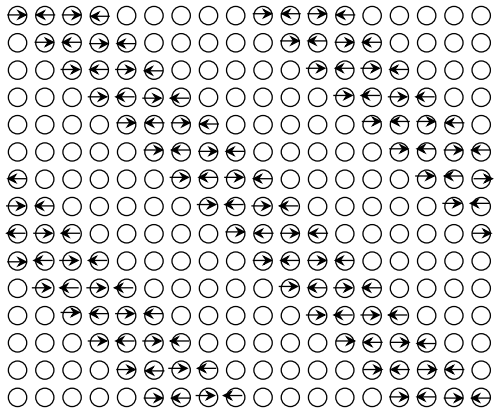

Fig. 4. A pictorial view of Cu-sites ordered in stripes. The circles with arrows are highly distorted CuO_2 planes while empty circles are undistorted CuO_2 planes (or Cu sites with small distortions).

In conclusion, the high k-resolution polarized EXAFS data, measured along the two orthogonal Cu–O–Cu bonds of the CuO_2 square plane, with a high signal to noise ratio are found to be encouraging to investigate microscopic anisotropy of atomic distribution in the two directions. The pair distribution of the Cu–O bonds along the two orthogonal directions shows significant differences, with preferential elongation and shortening of a part of the Cu–O bonds. We believe that the preferential tilting of the CuO_2 plane, giving anisotropy to the Cu–O bond distribution, is responsible for the evident asymmetry to the Fermi surface of the same system where $(\pi, 0)$ and $(0, \pi)$ points are different.

One of us (NLS) would like to thank the Science and Technology Agency (STA) for providing hospitality at the ETL during the experiments. This work is supported by "Istituto Nazionale di Fisica della Materia" (INFM) in the frame of the progetto "Stripes", by the "Ministero dell'Università e della

Ricerca Scientifica" (MURST) Programmi di Ricerca Scientifica di Rilevante Interesse Nazionale coordinated by R. Ferro, and by "Progetto 5% Superconduttività of Consiglio Nazionale delle Ricerche" (CNR).

References

1. see *e.g.*, K.A. Müller, in *Stripes & Related Phenomena*, edited by A. Bianconi, N.L. Saini (Kluwer/Plenum, New York, 2000).
2. J.B. Goodenough, J.S. Zhou, Nature **386**, 229 (1997) and references therein.
3. C.J. Stevens, D. Smith, C. Chen, J.F. Ryan, B. Podobnik, D. Mihailovic, G.A. Wagner, J.E. Evetts, Phys. Rev. Lett. **78**, 2212 (1997).
4. H. Kamimura, A. Sano, J. Superconductivity **10**, 279 (1997).
5. J. Ranninger, J. Superconductivity **10**, 285 (1997).
6. K.P. Sinha, Mod. Phys. Lett. B **12**, 805 (1998).
7. D. Mihailovich, K.A. Müller, *High T_c Superconductivity: Ten years after the Discovery (Nato ASI, Vol. 343)*, edited by E. Kaldis, E. Liarokapis, K.A. Müller (Dordrecht, Kluwer, 1996), p. 243.
8. E.S. Bozin, S.J.L. Billinge, G.H. Kwei, H. Takagi, Phys. Rev. B **59**, 4445 (1999) and references therein.
9. see *e.g.* a review on lattice effects, T. Egami, S.J.L. Billinge, Prog. Mater. Sci. **38**, 359 (1994).
10. P. Calvani, P. Dore, S. Lupi, A. Paolone, P. Maselli, P. Giura, B. Ruzicka, S.-W. Cheong, W. Sadowski, J. Superconductivity **10**, 293 (1997).
11. F. Cordero, C.R. Grandini, G. Cannelli, R. Cantelli, F. Trequattrini, M. Ferretti, Phys. Rev. B **57**, 8580 (1998).
12. G.-m. Zhao, M.B. Hunt, H. Keller, K.A. Muller, Nature (London) **385**, 236 (1997).
13. Bi Xiang-Xin, P.C. Eklund, Phys. Rev. Lett. **70**, 2625 (1993).
14. H.J. Kaufmann, E.K.H. Salje, Y. Yagil, O.V. Dolgov, J. Superconductivity **10**, 299 (1997); A.S. Alexandrov, A.M. Bratkovsky, N.F. Mott, E.H. Salje, Physica C **215**, 359 (1993).
15. M. Weger, J. Superconductivity **10**, 435 (1997).
16. A. Perali, C. Castellani, C. Di Castro, M. Grilli, Phys. Rev. B **54**, 16216 (1996).
17. A. Bianconi, in *Proc. of the Erice workshop, May 6-12, 1992, on Phase separation in cuprate superconductors*, edited by K.A. Müller, G. Benedek (World Scientific Pub., Singapore, 1993), p. 125.
18. J.B. Goodenough, J.S. Zhou, J. Superconductivity **10**, 309 (1997); J.S. Zhou, J.B. Goodenough, Phys. Rev. B **56**, 6288 (1997).
19. K.A. Müller, Guo-meng Zhao, K. Conder, H. Keller, J. Phys. Cond. Matter **10**, L291 (1998).
20. J. Ashkenazi, J. Superconductivity **10**, 379 (1997).
21. A. Lanzara, G.-m. Zhao, N.L. Saini, A. Bianconi, K. Conder, H. Keller, K.A. Müller, J. Phys. Cond. Matter **11**, L541 (1999).
22. D. Rubio Temprano, J. Mesot, S. Janssen, K. Conder, A. Furrer, H. Mutka, K.A. Müller, Phys. Rev. Lett. **84**, 1990 (2000).
23. J. Hofer, K. Conder, T. Sasagawa, Guo-meng Zhao, M. Willemin, H. Keller, K. Kishio, Phys. Rev. Lett. **84**, 4192 (2000) and references therein.
24. K.B. Garg, A. Bianconi, S. Della Longa, A. Clozza, M. de Santis, A. Marcelli, Phys. Rev. B **38**, 244 (1988).
25. J. Mustre de Leon, S.D. Conradson, I. Batistic, A.R. Bishop, Phys. Rev. Lett. **65**, 1675 (1990); J. Mustre de Leon, I. Batistic, A.R. Bishop, S.D. Conradson, S.A. Trugman, Phys. Rev. Lett. **68**, 3236 (1992) and references therein.
26. Z. Tan, J.I. Budnick, S. Luo, W.Q. Chen, S.-W. Cheong, A.S. Cooper, P.C. Cantfield, Z. Fisk, Phys. Rev. B **44**, 7008 (1991); Z. Tan, J.I. Budnick, C.E. Bouldin, J.C. Woicik, S.-W. Cheong, A.S. Cooper, G.P. Espinosa, Z. Fisk, Phys. Rev. B **42**, 1037 (1990).
27. A. Bianconi, C. Li, F. Campanella, S. Dell Longa, I. Pettiti, M. Pompa, S. Turtu, D. Udron, Phys. Rev. B **44**, 4560 (1991); A. Bianconi, C. Li, M. Pompa, Phys. Rev. B **45**, 4560 (1991).
28. H. Oyanagi, K. Oka, H. Unoki, Y. Nishihara, K. Murata, H. Yamaguchi, T. Matsushita, M. Tokumoto, Y. Kimura, J. Phys. Soc. Jpn **58**, 2896 (1989); H. Oyanagi, H. Kimura, T. Terashima, Y. Bando, J. Phys. Soc. Jpn **64**, 2563 (1995).
29. A. Bianconi, M. Lusignoli, N.L. Saini, P. Bordet, Å. Kvick, P.G. Radaelli, Phys. Rev. B **54**, 4310 (1996); A. Bianconi, N.L. Saini, T. Rossetti, A. Lanzara, A. Perali, M. Missori, H. Oyanagi, H. Yamaguchi, Y. Nishihara, D.H. Ha, Phys. Rev. B **54**, 12018 (1996).
30. A. Bianconi, N.L. Saini, A. Lanzara, M. Missori, T. Rossetti, H. Oyanagi, H. Yamaguchi, K. Oka, T. Ito, Phys. Rev. Lett. **76**, 3412 (1996).
31. A. Lanzara, N.L. Saini, A. Bianconi, J.L. Hazemann, Y. Soldo, F.C. Chou, D.C. Johnston, Phys. Rev. B **55**, 9120 (1997).
32. N.L. Saini, A. Lanzara, A. Bianconi, in *X-ray and Inner-Shell Processes*, *AIP Conference Proceedings* 389, edited by R.L. Johnson, H. Schmidt-Böcking, B.F. Sonntag (Woodbury, New York, 1997), p. 565.
33. N.L. Saini, A. Lanzara, H. Oyanagi, H. Yamaguchi, K. Oka, T. Ito, A. Bianconi, Phys. Rev. B **55**, 12759 (1997).
34. N.L. Saini, J. Avila, A. Bianconi, A. Lanzara, M.C. Asensio, S. Tajima, G.D. Gu, N. Koshizuka, Phys. Rev. Lett. **79**, 3467 (1997); N.L. Saini, A. Bianconi, A. Lanzara, J. Avila, M.C. Asensio, S. Tajima, G.D. Gu, N. Koshizuka, Phys. Rev. Lett. **82**, 2619 (1999).
35. N.L. Saini, J. Avila, M.C. Asensio, S. Tajima, G.D. Gu, N. Koshizuka, A. Lanzara, A. Bianconi, Phys. Rev. B **57**, R11101 (1998).
36. N.L. Saini, A. Lanzara, A. Bianconi, H. Oyanagi, Phys. Rev. B **58**, 11768 (1998).
37. H. Oyanagi, R. Shioda, Y. Kuwahara, K. Haga, J. Synchrotron Rad. **2**, 99 (1995); H. Oyanagi, *ibid.* **5**, 48 (1998).
38. *X Ray Absorption: Principle, Applications Techniques of EXAFS, SEXAFS and XANES*, edited by R. Prinz, D. Koningsberger (J. Wiley and Sons, New York 1988).
39. L. Tröger, D. Arvanitis, K. Baberschke, H. Michaelis, U. Grimm, E. Zschech, Phys. Rev. B **46**, 3283 (1992).
40. N.L. Saini, A. Lanzara, A. Bianconi, H. Oyanagi, H. Yamaguchi, K. Oka, T. Ito, Physica C **268**, 121 (1996).
41. A. Lanzara, N.L. Saini, M. Brunelli, F. Natali, A. Bianconi, P.G. Radaelli, S.-W. Cheong, Phys. Rev. Lett. **81**, 878 (1998).
42. R.J. McQueeney, Y. Petrov, T. Egami, M. Yethiraj, G. Shirane, Y. Endoh, Phys. Rev. Lett. **82**, 628 (1999).